Research Square

Preprints are preliminary reports that have not undergone peer review.
They should not be considered conclusive, used to inform clinical practice,
or referenced by the media as validated information.

Oxalate induces phosphatidylserine externalization, apoptosis, and crystal-cell adhesion in renal tubular epithelial cells through the ROS-ADAM17-Notch1 axis

Yan Ma
The First Affiliated Hospital of Harbin Medical University
Zhenyu Bi
The First Affiliated Hospital of Harbin Medical University
Feihong Yang
The First Affiliated Hospital of Harbin Medical University
Xiuguo Gan
ganxiuguo@qq.com
The First Affiliated Hospital of Harbin Medical University

Article

Keywords: ROS, calcium oxalate, kidney stones, ADAM17, Notch1 signaling pathway, crystal-cell adhesion

Posted Date: May 4th, 2026

DOI: https://doi.org/10.21203/rs.3.rs-9282701/v1

License: This work is licensed under a Creative Commons Attribution 4.0 International License.
Read Full License

Additional Declarations: No competing interests reported.

Version of Record: A version of this preprint was published at Scientific Reports on September 2nd, 2026. See the published version at https://doi.org/10.1038/s41598-026-69652-7.

Abstract

Background

Oxalate salts induce reactive oxygen species (ROS) generation, leading to phosphatidylserine (PS) externalization from renal tubule epithelial cells and the development of kidney stone. This research investigated the roles of ADAM17 (A Disintegrin and Metalloproteinase 17) and the Notch1 signaling pathway in oxalate-induced cell crystal adhesion through ROS-mediated mechanisms.

Methods

We treated HK-2 with sodium oxalate to establish a model of damage. ROS were measured using DCFH-DA fluorescence, and apoptosis and PS externalization were measured using flow cytometry. QPCR was applied to evaluate the mRNA of ADAM17 and Notch1, while western blot analysis was employed to assess their corresponding protein levels. Crystal adhesion assays were used to assess cell adherence to calcium oxalate crystals. The function of ADAM17 in oxalate-induced injury was examined by siRNA-mediated knockdown.

Results

Exposure to oxalate significantly elevated ROS generation, apoptotic incidence, PS externalization, and crystal adhesion in HK-2 cells. Moreover, oxalate exposure upregulated ADAM17 expression and activated the Notch1 signaling pathway. Antioxidant treatment reduces ADAM17 expression and inhibits Notch1 pathway activation. ADAM17 knockdown partially rescued ROS-induced apoptosis and PS externalization, reduced crystal adhesion, and suppressed Notch1 signaling.

Conclusion

Oxalate triggers apoptosis, PS externalization, and crystal cell adhesion in renal tubular epithelial cells through the ROS-ADAM17-Notch1 axis.

1. Introduction

Kidney stones, a widespread and highly prevalent urinary system disease, have a global incidence ranging from 1% to 15%[1]. The high incidence and recurrence of this disease pose major health and economic risks. The vast majority of kidney stones are calcium oxalate stones[2], yet their pathogenesis remains unclear. Therefore, in order to prevent kidney stones, investigating the pathological mechanisms behind the development of calcium oxalate renal stones holds significant importance..

A crucial element in the formation of calcium oxalate kidney stones involves the attachment of these crystals to renal tubular epithelial cell surfaces[3]. Oxalate exposure compromises renal tubule cells, impairing structure and activity, and fostering crystal accumulation[4–6]. When renal tubule cells are exposed to oxalate, oxidative stress is triggered, which is marked by the overproduction of ROS. This surge causes cellular damage, functional impairment, and apoptosis[7]. During apoptosis, PS redistributes to the outer membrane leaflet from its physiological inner localization, thereby exposing the negatively charged regions. Early studies indicated oxalate exposure triggers the generation of ROS, leading to the outward translocation of phosphatidylserine in renal tubular epithelial cells. The exposure of phosphatidylserine on the cell surface facilitates crystal adhesion, which in turn accelerates the progression of kidney stone formation[8]. However, the intrinsic mechanism of action is fuzzy.

Numerous previous researches have indicated that ROS promotes the expression and activation of a disintegrin and metalloproteinase 17(ADAM17) in cell models of various diseases[9–11]. ADAM17 is a protein pivotal in the development and release of various receptors[12]. It can activate TNF-α(Tumor Necrosis Factor-α) and EGFR(Epidermal growth factor receptor) ligands, promoting renal inflammation and fibrosis. Renal fibrosis leads to acute and chronic kidney injury[13–15], which is the pathologic basis of kidney stone[17].

Additionally, in a diabetic nephropathy cell injury model, Zhong et al. found that the promotion of ADAM17 transcription leads to unusual activation of the Notch1 signaling pathway[16]. This signaling pathway, being a crucial means of intercellular communication, is pivotal in the processes of cell growth and programmed cell death. It's especially key in sustaining the regular operation of renal tubular epithelial cells. In adult kidney tissues, the Notch pathway is expressed at low levels, however, it becomes activated in a variety of kidney diseases[18–20]. Upon activation, Notch1 binds to its ligand and is cleaved by ADAM17[21]. Subsequently, at the S3 site, the intracellular domain of Notch1 (NICD) is released into the nucleus, leading to the transcription of target genes involved in biological processes such as apoptosis[22]. One study reported that inhibiting the activation of Notch1 signaling through γ-secretase can reduce cell apoptosis by lowering the protein Bax and increasing Bcl-2, thereby offering protective effects against kidney injury[23]. Notch also regulates membrane phospholipid asymmetry through Atp8a2, which modulates the flipping of PS onto the cell membrane[24]. Therefore, we proposed that Notch1 pathway activation contributes to oxalate-induced apoptosis and phosphatidylserine externalization in HK-2 cells. PS flipping on the cell membrane and apoptosis are important pathological processes in oxalate-induced renal tubule epithelial cell stone formation[25, 26].

In the scope of this investigation, building upon our past work, we aimed to determine if high oxalate concentrations cause renal tubular epithelial cells to produce ROS. They then kick off the ADAM17-Notch1 signaling cascade, facilitating cell apoptosis, PS externalization, and crystal-cell adhesion. Our study aimed to investigate the cause of ROS-triggered PS externalization in HK2 cells and shed light on the mechanism that drives the development of calcium oxalate renal stones.

2. Materials and methods

2.1. Cell culture

HK-2 cells were from Cellverse (Shanghai, China). Cells were cultured in DMEM/F12 medium (Seven, China) supplemented with 1% penicillin-streptomycin (Beyotime, China) and 10% fetal bovine serum (BI, Israel), and incubated at 37℃ in an atmosphere containing 5% CO_2. After the cells had been passaged 3 times, we performed cell processing.

2.2. Cell grouping and treatment

1. 2.2.1. Three groups were established: control, OX, and PBN + OX. We treated the control group with complete culture medium. We treated the OX group with 1 mM sodium oxalate (Yuanye Bio, Shanghai, China) for 24 h. Lastly, cells in the PBN + OX group were pretreated with 4 mM PBN (N-tert-Butyl-α-phenylnitrone, MCE, USA) for 2 h, followed by 1 mM sodium oxalate treatment for 24 h.
2. 2.2.2. Three groups were established: si-NC, si-NC + OX, si-ADAM17, and si-ADAM17 + OX. We treated the si-NC and si-ADAM17 with complete culture medium. We treated si-NC + OX and si-ADAM17 + OX groups with 1 mM sodium oxalate for 24 h.

2.3. Cell transfection

SiRNAs suppress ADAM17 expression. SevenBio helped us design siRNA targeting ADAM17 (si-ADAM17#1 and si-ADAM17#2) and negative control (si-NC). At approximately 80% confluence of cells within 6-well plates, siRNA transfection was carried out using Lipofectamine3000 (Invitrogen) in accordance with the supplier's instructions.

2.4. Detection of intracellular ROS

After each group of cells has been processed, discard the spent medium in the six-well plates. After washing with phosphate buffered saline (PBS), serum-free medium containing DCFH-DA solution (10 μM, HY-D0940, MCE, USA) was added. Then, thorough mixing, the plates were placed in the incubator at 37°C for 30 min, followed by three washes with medium to wash out residual DCFH-DA. Cells were visualized and imaged using a fluorescence microscope (Zeiss, Germany), and the mean fluorescence intensity was assessed with ImageJ software to gauge the ROS concentrations.

2.5. qRT-PCR

We used a cDNA synthesis kit (SM134, SevenBio, China) to reverse transcribe total RNA extracted from HK-2 cells into cDNA. Real-time quantitative PCR was performed using 2× SYBR Green qPCR Master Mix II (SM143, SevenBio, China) on a real-time fluorescence quantitative PCR analyzer (FQD-96C, Bioer Technology, China), strictly following manufacturer protocols. The results were normalized using β-actin mRNA as the internal reference for qRT-PCR. The ΔCt value was calculated as ΔCt = Ct (target gene) - Ct (β-actin). A higher ΔCt value indicates a lower expression level of the target gene. The relative

expression levels of the genes were represented in the form of $2^{-\Delta\Delta Ct}$. The following primers (Table 1) were used.

Table 1
primers.

Notch1-F	**GGTGAACTGCTCTGAGGAGATC**
Notch1-R	GGATTGCAGTCGTCCACGTTGA
NICD-F	GCAGTTGT-GCTCCTGAAGAA
NICD-R	CGGGCG-GCCAGAAAC
Hes1-F	GGAAATGACAGTGAAGCACCTCC
Hes1-R	GAAGCGGGTCACCTCGTTCATG
ADAM17-F	AACAGCGACTGCACGTTGAAGG
ADAM17-R	CTGTGCAGTAGGACACGCCTTT
β- actin-F	CTC-CATCCTGGCCTCGCTGT
β- actin-R	GCT-GTCACCTTCACCGTTCC

2.6. Western blot

After treatment, the cells in each well of the six-well plate were ruptured using RIPA lysis buffer for protein extraction. Following SDS-PAGE separation, protein samples were electroblotted onto PVDF membranes (Merck, Germany). Following 2-hour blocking in 5% non-fat dry milk at RT (20–25°C), membranes were incubated with primary antibodies diluted in TBST.:

ADAM17 (1:500, WL04487, WanleiBio, China), Notch1 (1:1,000, CY5244, Abways, China), NICD (1:1,000, YP-Ab-12892, UpingBio, China), Hes1 (1:500, YP-Ab-07080, UpingBio, China), Bcl2 (1:500, WL01556, WanleiBio, China), Bax (1:2000, 50599-2-Ig, Proteintech, China), CD44 (Leukocyte differentiation antigen 44,1:2000, PTM-6106, PTM Bio, China), OPN (Osteopontin, 1:1000, WL00691, WanleiBio, China). The membranes were exposed to primary antibodies at 4°C for 16–18 hours, followed by triple TBST washes (10 min/wash). They were then exposed to a secondary antibody (1:10,000, SA00001-2/SA00001-1, Proteintech, China) at 25°C for 2 h. Proteins were detected using an ECL Chemiluminescent Substrate Kit (34580, Thermo Scientific, USA) and exposed to X-ray film. Finally, protein band quantification was performed using ImageJ, with relative expression levels normalized to β-actin loading controls.

2.7. Flow cytometry detection of cell apoptosis and PS externalization rate

Annexin V-FITC can bind to phosphatidylserine (PS), which is externalized during apoptosis, whereas propidium iodide (PI) can permeate the membranes of late apoptotic and necrotic cells. Therefore, Annexin V-FITC/PI double staining (SC123, SevenBio, China) was used to detect PS externalization and

differentiate between apoptosis and necrosis. In accordance with the manufacturer's instructions, the cells were rinsed twice using PBS and then digested with trypsin (SevenBio, China) that contained no EDTA. Following centrifugation, cells were resuspended in kit-supplied buffer, followed by addition of 5 μl Annexin V-FITC and 5 μl propidium iodide (PI) per tube with subsequent gentle mixing. Following 10-min incubation at 20–25°C, stained cells were analyzed on a BD FACScan flow cytometer. The results were analyzed using FlowJo_v10.8.1 software.

2.8. Cell crystal adhesion assay

After treatment, cells from each group were collected and seeded into 6-well plates at a density of 1×10^6 cells per well in serum-free medium. After 3–4 h incubation for complete adhesion, the medium was replaced with serum-free medium containing COM powder (100 μg/mL; HY-Y0262D, MCE, USA). Cells were exposed to COM powder at 37°C for 30 min. Post-incubation, they were rinsed three times with Hank's balanced salt solution (5 min/wash) to eliminate calcium oxalate crystals that had not adhered. Crystal-cell adhesion was documented via phase-contrast microscopy. Subsequently, bound crystals were dissolved with 10% HCl (2 mL/well), and lysate Ca^{2+} concentrations were quantified using a calcium assay kit (Beyotime, China) per manufacturer's protocol. The level of crystal cell adhesion was calculated as follows:

Crystal cell adhesion ability = Calcium ion concentration in the treatment group - Calcium ion concentration in the corresponding treatment group without COM crystal powder.

3. Statistical analysis

Each experiment was conducted three times, and the resulting data were processed using GraphPad Prism 10.1.2 software. Outcomes are expressed as the mean±standard error of the mean (SEM). For comparisons between two separate groups, Student's t-tests were applied, while a one-way analysis of variance (ANOVA) was utilized to analyze differences across multiple groups.Statistical significance was set at $p < 0.05$.

4. Results

4.1. PBN pretreatment alleviated oxalate-induced ROS generation

PBN (N-tert-Butyl-α-phenylnitrone) was employed to assess ROS involvement in oxalate-triggered PS externalization, crystal adhesion and apoptosis. Relative to controls, OX group exhibited markedly elevated ROS levels. PBN pretreatment substantially attenuated oxalate-induced oxidative stress (Fig. 1).

4.2. Inhibition of ROS production alleviated oxalate-induced cell apoptosis and PS externalization

We assessed the pro-apoptotic effects of oxalate on HK-2 cells. Flow cytometric analysis demonstrated significantly elevated apoptotic rates and phosphatidylserine exposure in oxalate-exposed HK-2 cells (OX group) (Fig. 2B). Bcl-2 and Bax, which are key apoptotic proteins, showed significant changes (Fig. 2A). However, PBN pretreatment significantly reduced the oxalate-induced apoptosis and PS externalization.

4.3. Inhibition of ROS production reduces oxalate-induced crystal-cell adhesion and related adhesion molecule expression

The ability of cells to adhere to crystals was assessed using a crystal-cell adhesion assay and the expression of OPN and CD44 (Fig. 3B). HK-2 cells treated with high oxalate concentrations exhibited an increased expression of adhesion molecules, and COM crystals adhered more to the cell surface. However, PBN pretreatment markedly attenuated HK-2 cell adhesion capacity to COM crystals. (Fig. 3A).

4.4. Oxalate increases ADAM17 expression through ROS-mediated activation of the Notch1 signaling pathway

Studies have shown that oxidative stress promotes ADAM expression of ADAM17. Consequently, we supposed that high-concentration oxalate treatment of HK-2 would increase ADAM17 expression mediated by oxidative stress. As shown in Fig. 4, western blot and qPCR demonstrated that oxalate treatment significantly elevated the levels of ADAM17, Notch1, NICD, and Hes1 in HK-2 cells. Moreover, ROS partially suppressed ADAM17 expression and Notch1 pathway activation.

4.5. ADAM17 knockdown alleviates oxalate-induced cell apoptosis, PS externalization, and crystal-cell adhesion

Next, we investigated whether silencing ADAM17 could improve oxalate-induced crystal cell adhesion and cell apoptosis using siRNA to knockdown ADAM17 expression. Then we confirmed the knockdown efficiency by western blot (Fig. 5A). In the crystal cell adhesion experiment, the adhesion of COM crystals to the surface of HK-2 cells was significantly diminished following the silencing of ADAM17 (Fig. 7A). Flow cytometry analysis revealed that the knockdown of ADAM17 reversed oxalate-induced apoptosis (Fig. 6A). At the protein level, the si-ADAM17 + OX group exhibited a significant reduction in the pro-apoptotic protein Bax compared with the si-nc + OX group. Contrarily, the level of Bcl-2, an anti-apoptotic protein, was notably increased (Fig. 6B). Knockdown of ADAM17 also inhibited oxalate-induced elevation of OPN and CD44 (Fig. 7B). These results suggest that ADAM17 knockdown not only inhibits oxalate-induced crystal cell adhesion but also attenuates cell damage by modulating apoptosis-related proteins.

4.6. ADAM17 knockdown partially inhibits the activation of the Notch1 pathway induced by oxalate

To clarify the role of ADAM17 knockdown on the regulation of Notch1 signaling pathway activity under oxalic acid stress, our research further measured the expression changes of the key signaling molecule NICD and its downstream target gene Hes1. HK-2 cells that had been transfected with si-NC or si-ADAM17 were subjected to treatment with 1 mM sodium oxalate, and western blot was utilized to analyze the protein expression levels of NICD and Hes1. As shown in the results (Fig. 8A), when compared with the si-nc + OX group, the expression levels of both NICD and Hes1 in the si-ADAM17 + OX group were importantly decreased (*$p < 0.05$), suggesting that ADAM17 knockdown effectively inhibited the activation of Notch1 signaling pathway triggered by oxalate stimulation.

5. Discussion

Crystal-cell adhesion plays a critical role in kidney stone formation. Although the mechanisms underlying crystal cell adhesion remain unclear, growing evidence suggests that high concentrations of oxalate induce oxidative stress in renal tubular epithelial cells, generating amounts of ROS, damaging epithelial cells, and subsequently promoting stone formation[27–29].Antioxidants are capable of reducing harm to renal tubular epithelial cells, and they can also decrease the adhesion and accumulation of these crystals[6, 7, 30]. Furthermore, our prior study confirmed that oxalate-induced ROS generation leads to PS externalization from renal tubular epithelial cell membranes. The negatively charged phosphatidylserine present on the cell surface functions as an anionic molecule, playing a mediating role in the adhesion of calcium oxalate monohydrate crystals[8]. We confirmed that the oxalate treatment of HK-2 significantly increased ROS production, promoted apoptosis and PS externalization, and enhanced the adhesion of crystals.

Emerging evidence highlights that ADAM17 mediates the proteolytic shedding of extracellular domains from diverse cytokines, cell adhesion molecules, receptors, ligands, and enzymes.[31–34]. In the kidney, ADAM17 is significantly elevated in the kidney during acute and chronic kidney injury[35]. However, no studies have explored the direct relationship between ADAM17 and oxalate-induced damage to renal tubular epithelial cells. In HK-2 cells exposed to oxalate, the ADAM17 expression showed a marked increase, with this rise being associated with higher ROS concentrations. The level of ADAM17 was markedly reduced using PBN to inhibit ROS production. Additionally, siRNA-mediated ADAM17 knockdown significantly decreased oxalate-induced apoptosis and PS externalization, further reducing calcium oxalate crystal adhesion. These findings suggest that the ROS-mediated upregulation of ADAM17 contributes to oxalate-induced renal tubular epithelial cell damage and COM crystal adhesion.

Studies have demonstrated that inhibiting Notch1 signaling can reduce apoptosis by regulating Bax and Bcl2, thereby exerting protective effects following kidney injury[23]. In the present study, an investigation was conducted into the impacts of oxalate on the Notch1 signaling pathway within HK-2 cells. Our results showed that oxalate treatment at high concentrations significantly increased the expression of Notch1, elevated NICD production, and upregulated the mRNA and protein levels of downstream genes such as Hes1. These results indicate that the ROS-driven increase in ADAM17 expression plays a role in

renal tubular epithelial cell injury and COM crystal attachment caused by oxalate. Notch1 activation requires cleavage of the S2 site by ADAM17. ADAM17 knockdown inhibited oxalate-induced activation of the Notch1 pathway, thereby reducing phosphatidylserine externalization. Additionally, regulation of Bax and Bcl2 expression suppressed oxalate-induced apoptosis, thereby decreasing the adhesion of COM crystals.

Prior researches have suggested that stimulation with oxalate or COM crystals increases the expression of CD44 and OPN in renal tubular epithelial cells, thereby promoting crystal adhesion and retention[36–38]. Similarly, our experiments demonstrated that CD44 and OPN expression increased in HK-2 cells treated with high oxalate concentrations. The antioxidant PBN inhibited oxalate-induced upregulation of CD44 and OPN. Additionally, ADAM17 knockdown significantly reduced oxalate-induced CD44 and OPN expression. This suggests that ADAM17 knockdown partially reduces calcium oxalate crystal adhesion by suppressing CD44 and OPN expression.

Although this study reveals the role of ADAM17 in oxalate-induced cellular damage, it has several limitations. First, although the HK-2 cell model provides valuable experimental data, it does not fully replicate the complex pathological conditions involved in kidney stone formation in humans. Second, the concentration and duration of the oxalate treatment used in this study may not have accurately reflected the physiological environment of patients with kidney stones. Future studies should optimize the experimental designs to explore more clinically relevant treatment protocols.

6. Conclusion

Our results suggested that oxalate induces renal tubular epithelial cell damage by generating ROS, leading to apoptosis and phosphatidylserine externalization. Oxalate activates the Notch1 signaling pathway, promoting apoptosis and PS externalization, which are mediated by the cleavage of ADAM17. Notably, oxalate-induced cell injury increases the expression of adhesion molecules, such as CD44 and OPN, which further facilitates the attachment of calcium oxalate crystals to the renal epithelium. In contrast, inhibiting ROS production or silencing ADAM17 effectively reduces the expression of these adhesion molecules, suggesting a potential therapeutic approach to mitigate kidney stone formation.

In summary, our research explored the damaging effects of high concentrations of oxalate on renal tubular epithelial cells and revealed potential mechanisms involving ROS, ADAM17, and the Notch1 signaling pathway in calcium oxalate stone formation. Our findings provide new theoretical insights into the role of oxalate in kidney stone formation and suggest potential therapeutic strategies to mitigate this process.

Declarations

Author contributions

Ma, Yan:Validation,Investigation,Data Analysis,Writing,Original Draft

Bi,Zhengyu:Combined Pictures;

Yang,Feihong:Investigation;

Gan, Xiuguo:Conceptualization,Methodology,Resources,Writing,Review & Editing;

Competing interests

The authors declare that there are no financial or non-financial conflicts of interest that could influence the interpretation or presentation of the results in this study.

Data Availability Statement

The data supporting the findings of this study are available within the paper and its Supplementary Information files.

Funding

This study was supported by the Natural Science Foundation of Heilongjiang Province(Grant no.LH2022H036).

References

1. Wang, Z., Zhang, Y., Zhang, J., Deng, Q. & Liang, H. Recent advances on the mechanisms of kidney stone formation (Review). *Int. J. Mol. Med.* **48**, 149 (2021).
2. Ming, S. et al. Oxalate-induced apoptosis through ERS-ROS-NF-κB signalling pathway in renal tubular epithelial cell. *Mol. Med.* **28**, 88 (2022).
3. Ye, Q. L. et al. Sirt1 inhibits kidney stones formation by attenuating calcium oxalate-induced cell injury. *Chem. Biol. Interact.* **347**, 109605 (2021).
4. Qin, B. et al. Losartan Ameliorates calcium oxalate-induced elevation of stone-related proteins in renal tubular cells by inhibiting NADPH oxidase and oxidative stress. Oxid Med Cell Longev. 2018:1271864. (2018).
5. Deng, J. W. et al. Mechanism of porphyra yezoensis polysaccharides in inhibiting hyperoxalate-induced renal injury and crystal deposition. *J. Agric. Food Chem.* **72** (12), 6372–6388 (2024).
6. Heng, B. L., Wu, F. Y., Tong, X. Y., Zou, G. J. & Ouyang, J. M. Corn silk polysaccharide reduces the risk of kidney stone formation by reducing oxidative stress and inhibiting COM crystal adhesion and aggregation. *ACS Omega*. **9**, 19236–19249 (2024).
7. Lu, H. et al. Rosiglitazone suppresses renal crystal deposition by ameliorating tubular injury resulted from oxidative stress and inflammatory response via promoting the Nrf2/HO-1 pathway and shifting macrophage polarization. Oxid Med Cell Longev. 2021:5527137. (2021).
8. Yu, S. L. et al. Oxalate impairs aminophospholipid translocase activity in renal epithelial cells via oxidative stress: implications for calcium oxalate urolithiasis. *J. Urol.* **186**, 1114–1120 (2011).

9. Moreno-Càceres, J. et al. Caveolin-1-dependent activation of the metalloprotease TACE/ADAM17 by TGF-β in hepatocytes requires activation of Src and the NADPH oxidase NOX1. *FEBS J.* **283**, 1300–1310 (2016).
10. Zeng, S. Y. et al. Upregulation of Nox4 promotes angiotensin II-induced epidermal growth factor receptor activation and subsequent cardiac hypertrophy by increasing ADAM17 expression. *Can. J. Cardiol.* **29**, 1310–1319 (2013).
11. Li, T. M. et al. The interferon-rich skin environment regulates Langerhans cell ADAM17 to promote photosensitivity in lupus. *Elife* **13**, e85914 (2024).
12. Jiang, N. et al. Inhibition of ADAM17 attenuates high glucose-induced angiogenesis and inflammation in endothelial cells partly through down-regulation of GRO-α/CXCR2 expression: implications in peritoneal dialysis. *Clin. Exp. Nephrol.* **28**, 1232–1240 (2024).
13. Kefaloyianni, E. et al. ADAM17 substrate release in proximal tubule drives kidney fibrosis. *JCI Insight*. **1**, e87023 (2016).
14. Perna, A. F. et al. ADAM17, a new player in the pathogenesis of chronic kidney disease-mineral and bone disorder. *J. Ren. Nutr.* **27**, 453–457 (2017).
15. Tang, J. et al. Neutrophil and macrophage cell surface colony-stimulating factor 1 shed by ADAM17 drives mouse macrophage proliferation in acute and chronic inflammation. *Mol. Cell. Biol.* **38**, e00103–e00118 (2018).
16. Zhong, W. et al. ASH2L-mediated H3K4me3 drives diabetic nephropathy through HIPK2 and Notch1 pathway. *Transl Res.* **264**, 85–96 (2024).
17. Liu, Y. et al. Telmisartan inhibits oxalate and calcium oxalate crystal-induced epithelial-mesenchymal transformation via PPAR-γ-AKT/STAT3/p38 MAPK-Snail pathway. *Life Sci.* **241**, 117108 (2020).
18. Zhu, Q. Q. et al. EGCG targeting Notch to attenuate renal fibrosis via inhibition of TGFβ/Smad3 signaling pathway activation in streptozotocin-induced diabetic mice. *Food Funct.* **11**, 9686–9695 (2020).
19. Marquez-Exposito, L. et al. Deletion of delta-like 1 homologue accelerates renal inflammation by modulating the Th17 immune response. *FASEB J.* **35**, e21213 (2021).
20. Song, B. F. et al. Overexpression of sirtuin 1 attenuates calcium oxalate-induced kidney injury by promoting macrophage polarization. *Int. Immunopharmacol.* **121**, 110398 (2023).
21. Alabi, R. O., Lora, J., Celen, A. B., Maretzky, T. & Blobel, C. P. Analysis of the conditions that affect the selective processing of endogenous notch1 by ADAM10 and ADAM17. *Int. J. Mol. Sci.* **22**, 1846 (2021).
22. Li, D., Xu, D., Zhang, Y., Chen, P. & Xie, J. Effect of Notch1 signaling on cellular proliferation and apoptosis in human laryngeal carcinoma. *World J. Surg. Oncol.* **20**, 262 (2022).
23. Soni, H., Matthews, A. T., Pallikkuth, S., Gangaraju, R. & Adebiyi, A. γ-secretase inhibitor DAPT mitigates cisplatin-induced acute kidney injury by suppressing Notch1 signaling. *J. Cell. Mol. Med.* **23** (1), 260–270 (2019).

24. Ishifune, C. et al. Regulation of membrane phospholipid asymmetry by Notch-mediated flippase expression controls the number of intraepithelial TCRαβ + CD8αα + T cells. *PLoS Biol.* **17**, e3000262 (2019).
25. Liang, H. et al. Based on network pharmacology, the mechanism of Dioscin in alleviating renal tubular epithelial cell injury induced by calcium oxalate crystals was explored. *Urolithiasis* **53**, 3 (2024).
26. Gan, X. G., Xu, H. T. & Wang, Z. H. Phosphatidylserine eversion regulated by phospholipid scramblase activated by TGF-β1/Smad signaling in the early stage of kidney stone formation. *Urolithiasis* **50**, 11–20 (2022).
27. Albert, A., Paul, E., Rajakumar, S. & Saso, L. Oxidative stress and endoplasmic stress in calcium oxalate stone disease: the chicken or the egg. *Free Radic Res.* **54**, 244–253 (2020).
28. Chaiyarit, S. & Thongboonkerd, V. Mitochondrial dysfunction and kidney stone disease. *Front. Physiol.* **11**, 566506 (2020).
29. Cao, W., Zhang, J., Yu, S., Gan, X. & An, R. N-acetylcysteine regulates oxalate induced injury of renal tubular epithelial cells through CDKN2B/TGF-β/SMAD axis. *Urolithiasis* **52**, 46 (2024).
30. Gao, M. et al. Inhibitory effect of Incarvillea diffusa Royle extract in the formation of calcium oxalate nephrolithiasis by regulating ROS-induced Nrf2/HO-1 pathway in rats. *J. Ethnopharmacol.* **325**, 117619 (2024).
31. Kaneko, T. et al. Regulation of osteoarthritis development by ADAM17/Tace in articular cartilage. *J. Bone Min. Metab.* **40**, 196–207 (2022).
32. Saad, M. I. et al. Blockade of the protease ADAM17 ameliorates experimental pancreatitis. *Proc. Natl. Acad. Sci. U S A*. **119**, e2213744119 (2022).
33. Sisto, M. & Lisi, S. Updates on inflammatory molecular pathways mediated by ADAM17 in autoimmunity. *Cells* **13**, 2092 (2024).
34. Düsterhöft, S., Lokau, J. & Garbers, C. The metalloprotease ADAM17 in inflammation and cancer. *Pathol. Res. Pract.* **215**, 152410 (2019).
35. Meyer-Schwesinger, C., Seipold, L. & Saftig, P. Ectodomain shedding by ADAM proteases as a central regulator in kidney physiology and disease. *Biochim. Biophys. Acta Mol. Cell. Res.* **1869**, 119165 (2022).
36. Wang, B., He, G., Xu, G., Wen, J. & Yu, X. miRNA-34a inhibits cell adhesion by targeting CD44 in human renal epithelial cells: implications for renal stone disease. *Urolithiasis* **48**, 109–116 (2020).
37. Yang, X. et al. Metformin prevents nephrolithiasis formation by inhibiting the expression of OPN and MCP-1 in vitro and in vivo. *Int. J. Mol. Med.* **43**, 1611–1622 (2019).
38. Gan, Q. Z., Sun, X. Y. & Ouyang, J. M. Adhesion and internalization differences of COM nanocrystals on Vero cells before and after cell damage. *Mater. Sci. Eng. C Mater. Biol. Appl.* **59**, 286–295 (2016).

Figures

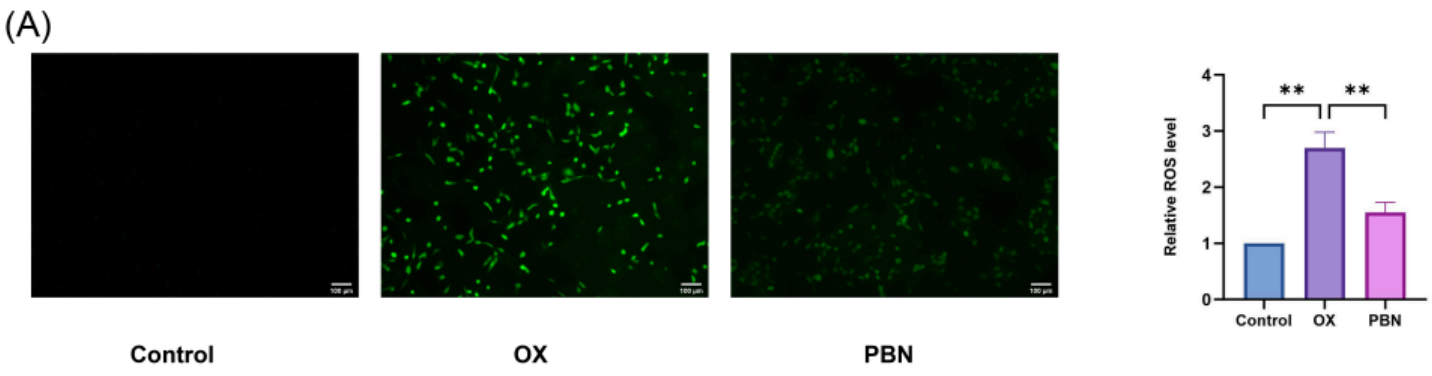


Figure 1

PBN pretreatment alleviated oxalate-induced ROS production. After treatment of HK-2 cells according to the respective groups, cells were collected for subsequent experiments. (A) DCFH-DA (10 μM) staining of HK-2 cells enabled quantification of cellular ROS levels via mean fluorescence intensity. Magnification: 100×. The fluorescence intensity was used to indirectly reflect the cellular ROS levels. *P<0.05, **P<0.01

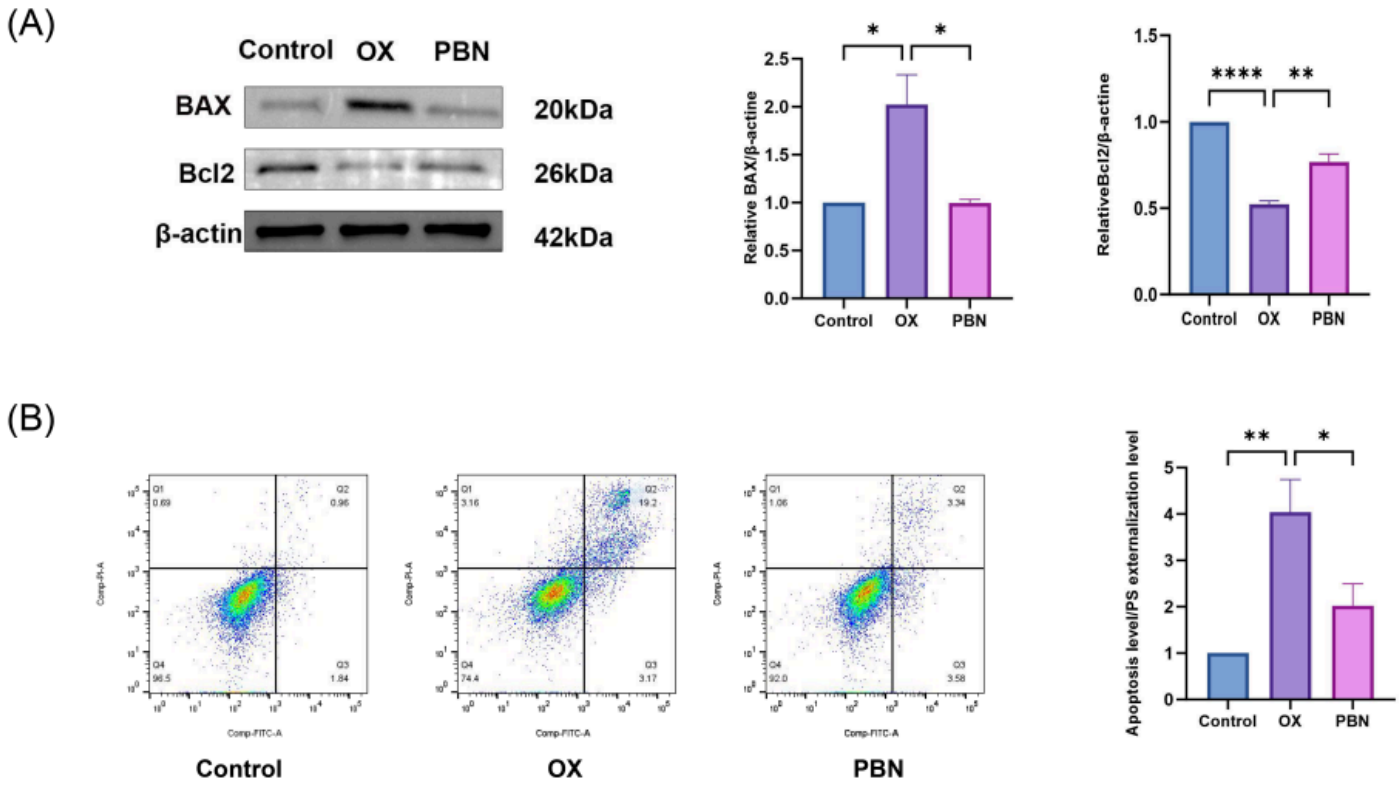


Figure 2

Inhibition of ROS production alleviates oxalate-induced cell apoptosis and PS externalization. After treating HK-2 cells according to the respective groups, the cells were collected for subsequent

experiments. (A) The expression of Bax and Bcl-2 were measured by Western blot. (B) Annexin V-PI double staining experiment and flow cytometry were utilized to evaluate cellular apoptosis and phosphatidylserine externalization metrics. *P<0.05, **P<0.01, ****P<0.0001

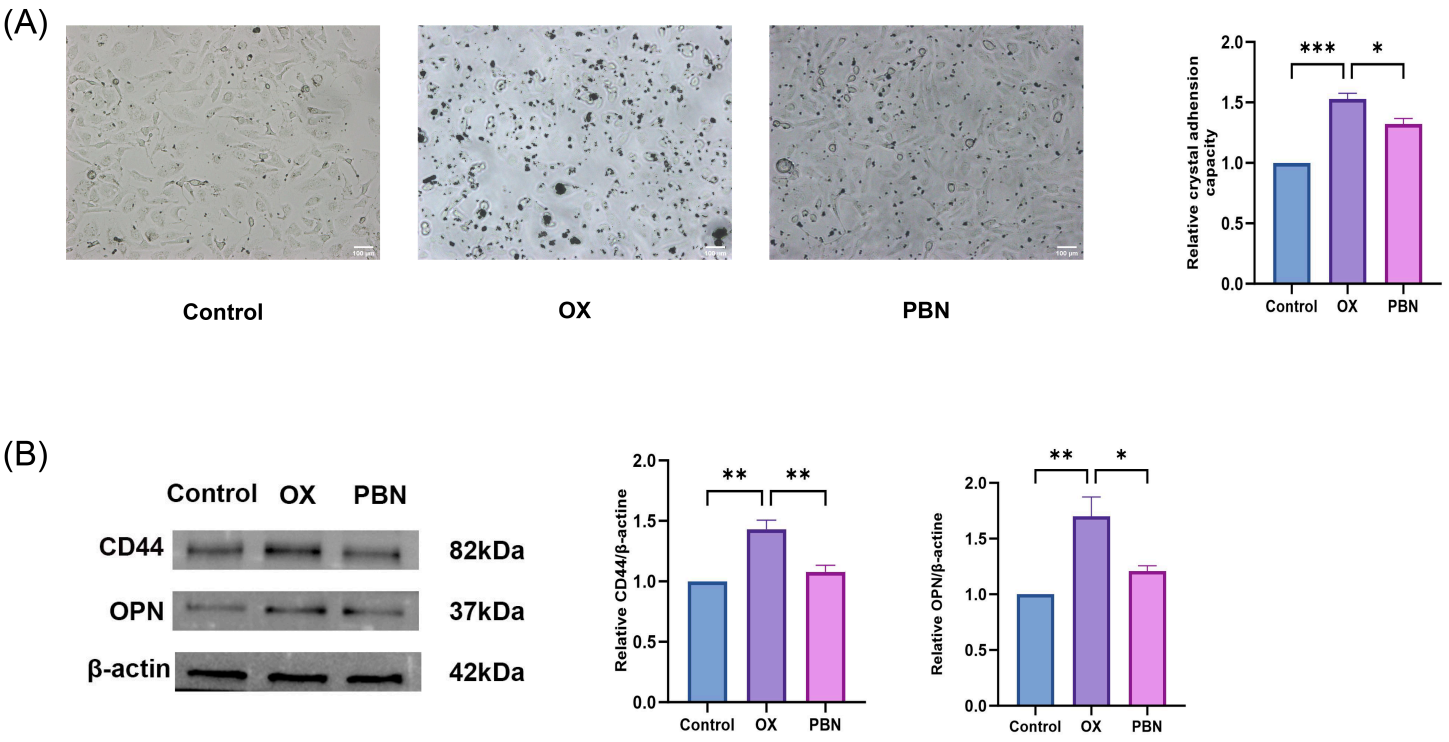


Figure 3

Inhibition of ROS generation reduces oxalate-induced crystal-cell adhesion and the expression level of adhesion molecules. According to the groupings, cells were collected for subsequent experiments.(A) Crystal-cell adhesion was observed under a light microscope to evaluate COM adhesion. The crystal-cell adhesion ability was quantified by measuring the concentration of Ca^{2+} in the supernatant using a calcium ion detection kit. (B) Western blot analysis was conducted to determine the expression levels of CD44 and OPN, which are proteins associated with cell adhesion. *P<0.05, **P<0.01, ***P<0.001

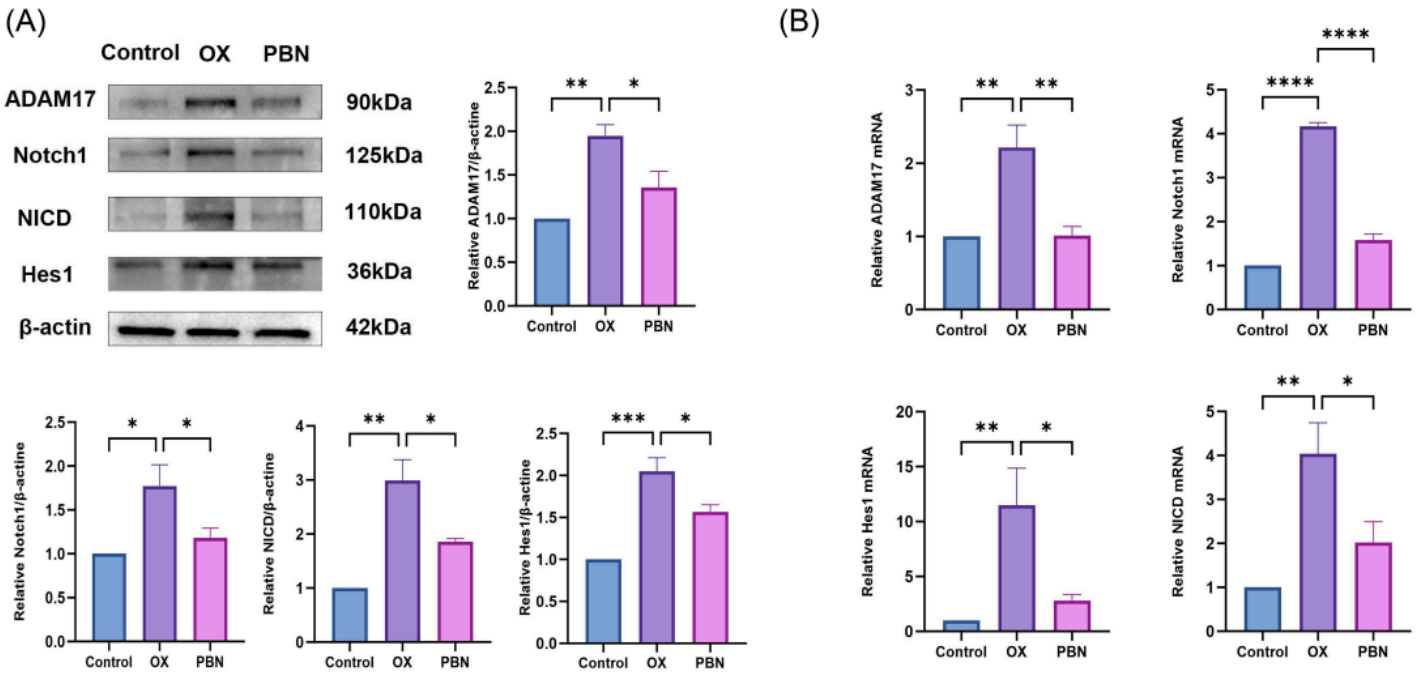


Figure 4

Oxalate increases ADAM17 expression and activates the Notch1 signaling pathway through ROS mediation. After treating HK-2 cells according to the experimental groups, cells were collected for subsequent experiments. **(A)** Western blot was employed to examine ADAM17 as well as the Notch1 signaling pathway. **(B)** We employed qPCR to determine the mRNA expression levels of ADAM17 and other genes associated with the Notch1 pathway. *P<0.05, **P<0.01, ***P<0.001, ****P<0.0001

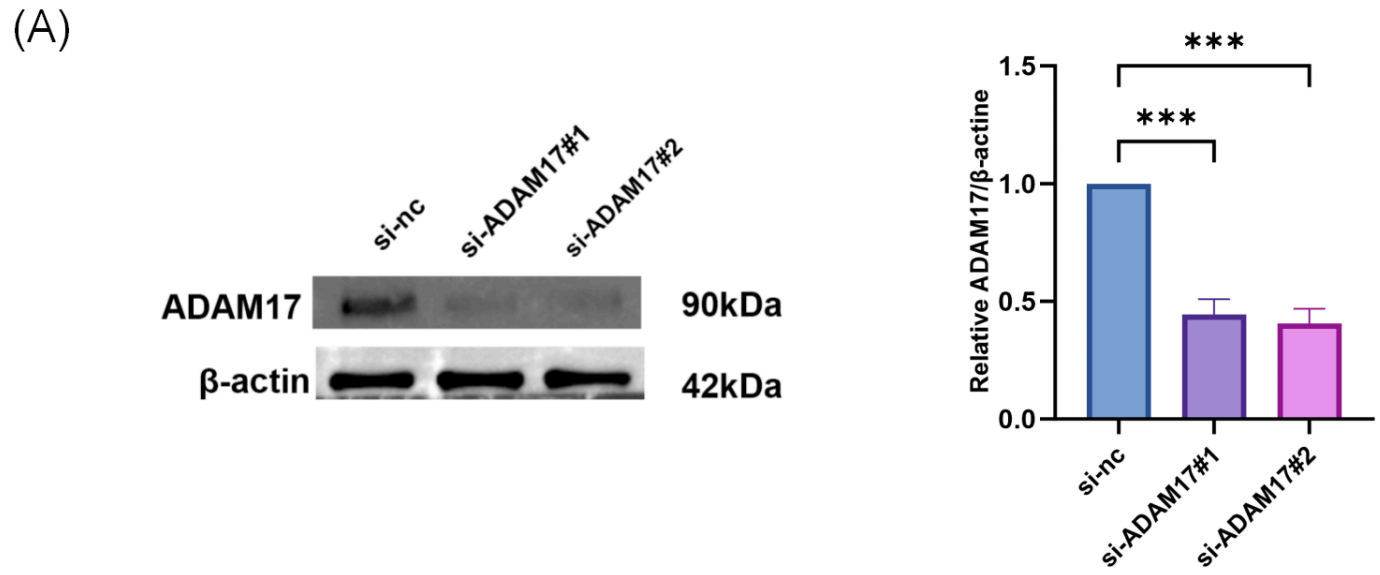


Figure 5

Successful knockdown of ADAM17 in HK-2. For the purpose of knocking down ADAM17 expression, we transfected si-ADAM17 in HK-2. The transfection efficiency was validated 72 h post-transfection. (A) We used western blot to assess the efficiency of knockdown. The loading control was β-actin. ***P<0.001

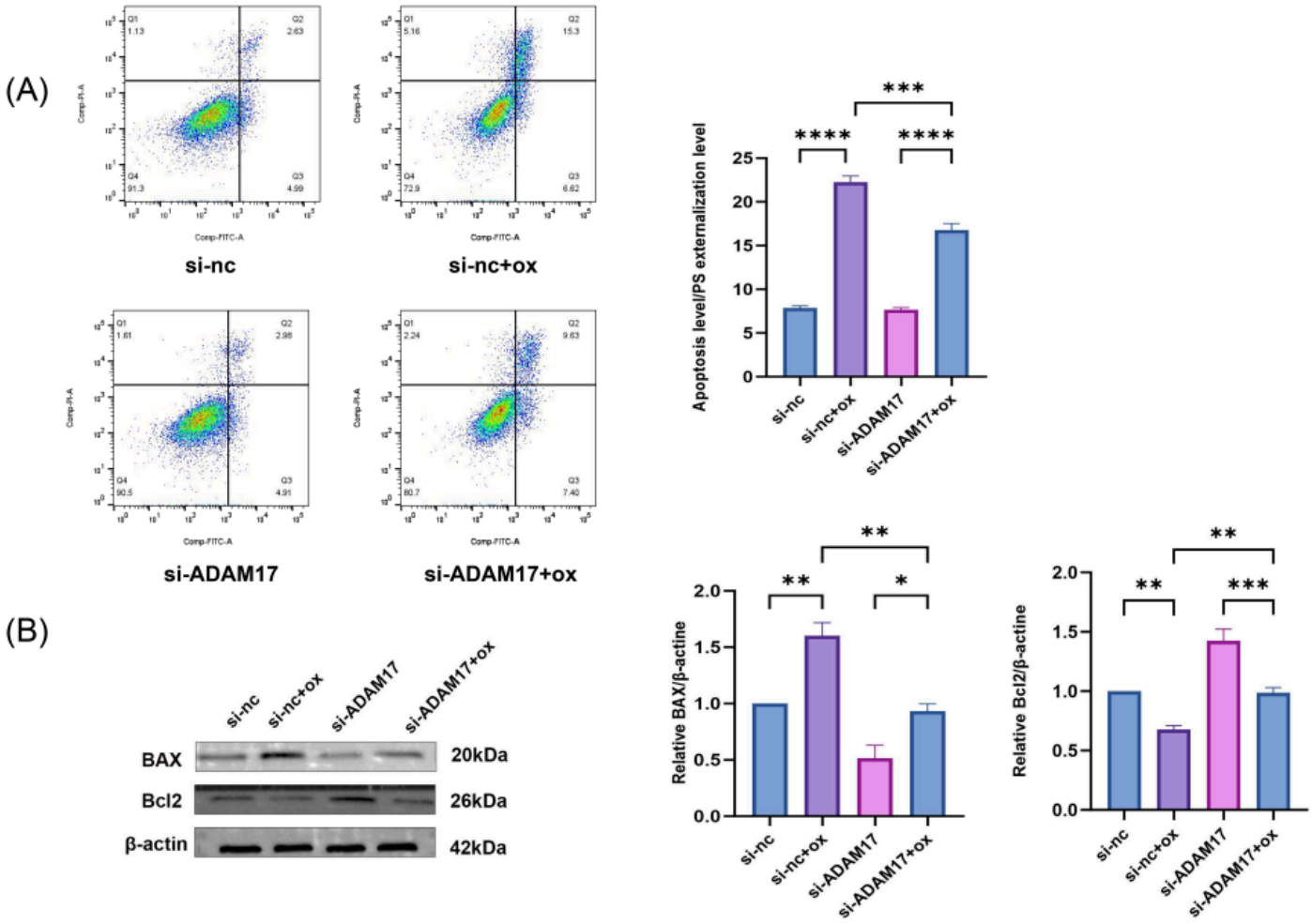


Figure 6

ADAM17 knockdown mitigates oxalate-induced cell apoptosis and PS externalization. After transfection, the cells were grouped and processed for subsequent experiments. (A) Annexin V-PI double staining combined with flow cytometry was employed to examine cell apoptosis and the levels of PS externalization. (B) Levels of BAX and Bcl2 proteins, which are related to cell apoptosis, were measured using Western blot assays to determine their expression. *P<0.05, **P<0.01, ***P<0.001, ****P<0.0001

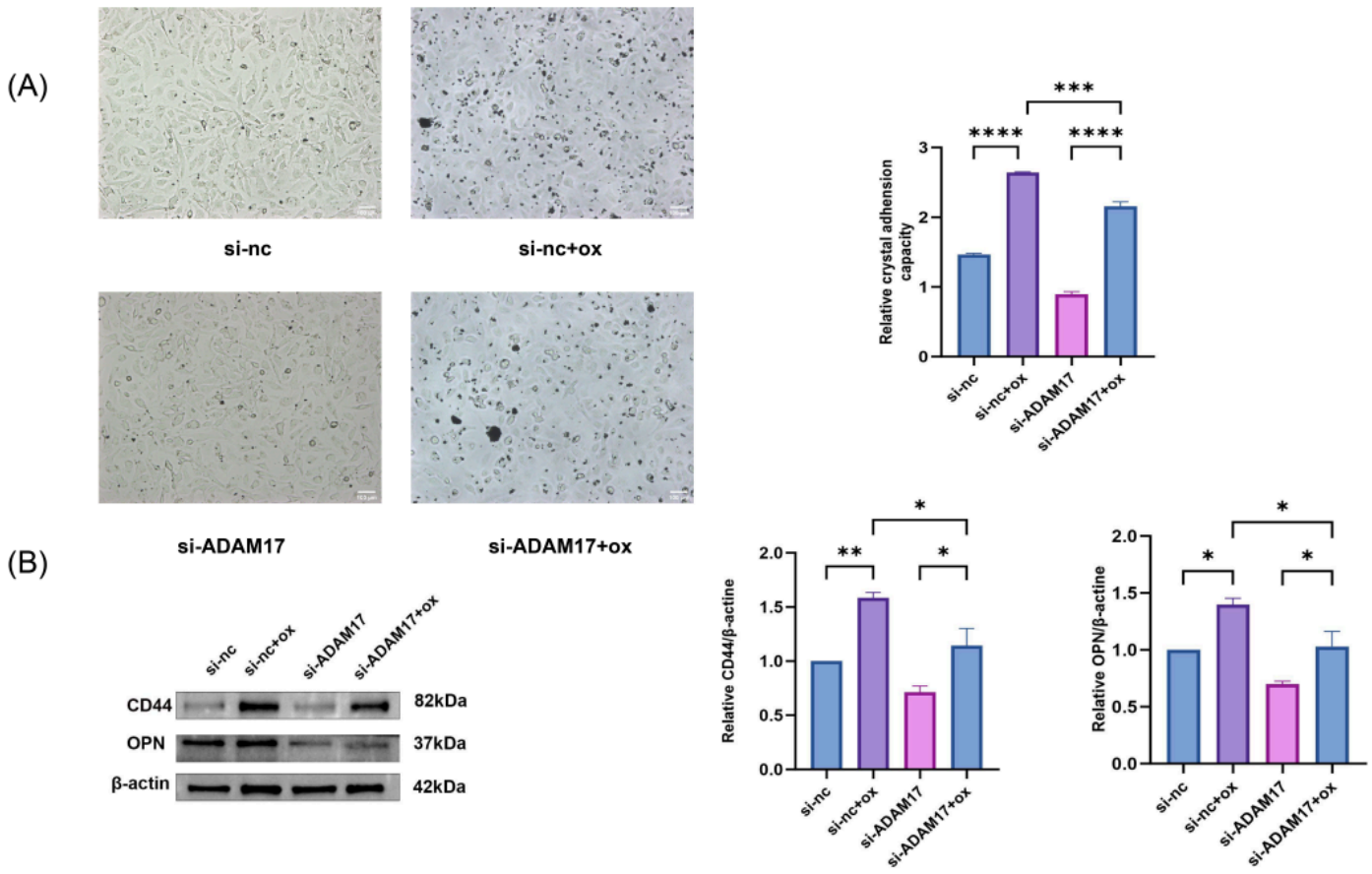


Figure 7

ADAM17 knockdown alleviates oxalate-induced crystal-cell adhesion and expression of adhesion-related proteins. (A) Crystal-cell adhesion was observed under a light microscope, and the level of crystal-cell adhesion was quantified by measuring the Ca^{2+} concentration in the supernatant using a calcium ion detection kit. (B) The expression levels of CD44 and OPN proteins, which take part in cell adhesion processes, were investigated via Western blot analysis. *P<0.05, **P<0.01, ***P<0.001

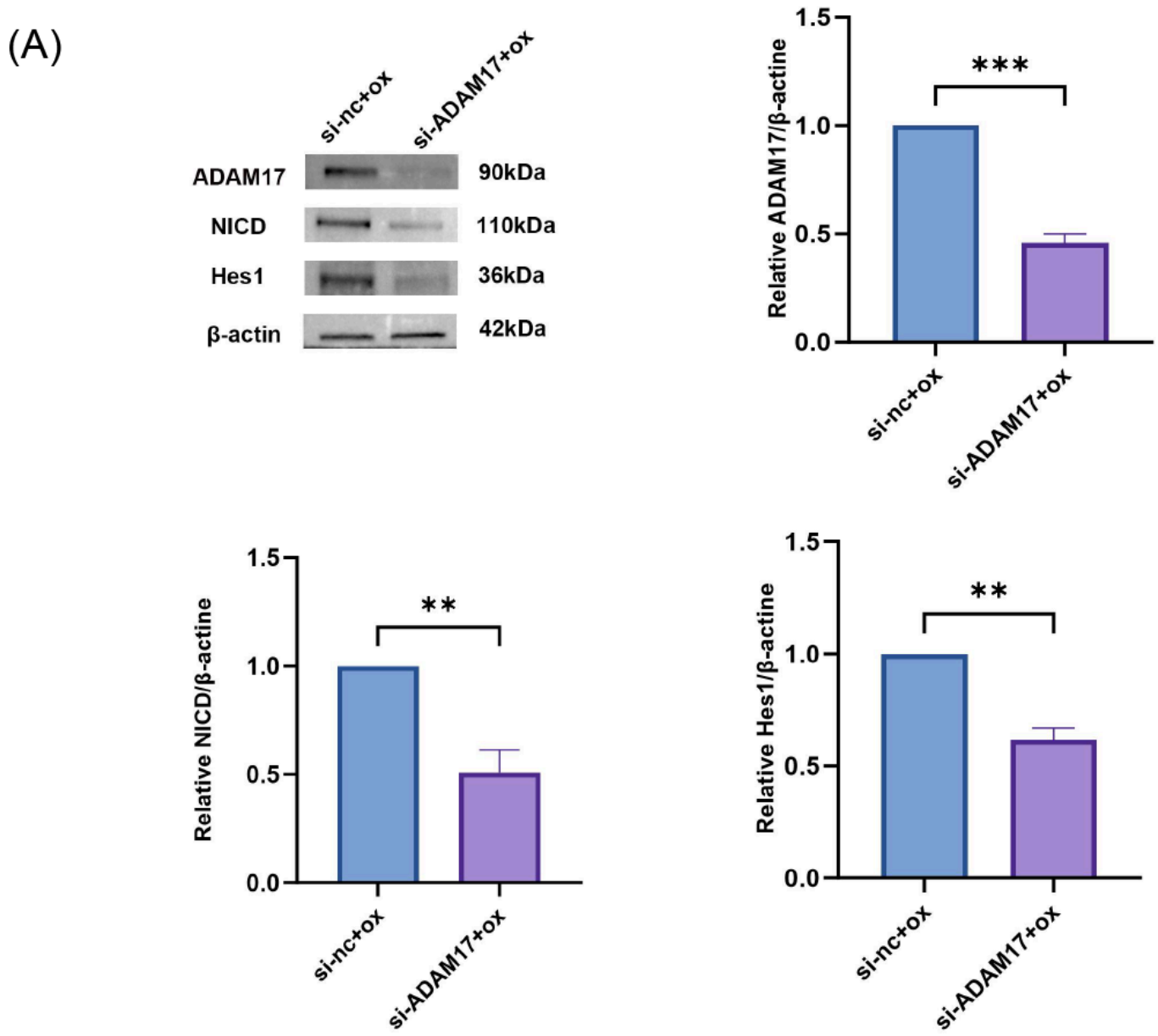


Figure 8

Knockdown of ADAM17 inhibited oxalic acid-induced activation of the Notch1 signaling pathway. Si-nc and si-ADAM17 were respectively transfected in HK-2 cells, Then the cells were treated with oxalic acid for a 24-hour period. Subsequently, western blot analysis was employed to determine the expression levels of ADAM17, NICD, and Hes1 in the cells individually. **P<0.01, ***P<0.001

Supplementary Files

This is a list of supplementary files associated with this preprint. Click to download.

- wbrawfigure.pdf